www.springer.com/41230
https://doi.org/10.1007/s41230-023-2183-6

Effect of Ce on microstructure and mechanical properties of Mg-Zn-Ce magnesium alloys

Hong-fei Wu[1, 2], *Wen-xin Hu[1, 2], Shao-bo Ma[1, 2], Zheng-hua Yang[1, 2], Wei Wang[1, 2], Feng Liu[1, 2], and Wei He[1, 2]

1. State Key Laboratory of Baiyunobo Rare Earth Resource Researches and Comprehensive Utilization, Baotou 014030, Inner Mongolia, China

2. Baotou Research Institute of Rare Earths, Baotou 014030, Inner Mongolia, China

Abstract: The Mg-6Zn alloy with different contents of Ce was prepared by the gravity casting method, and then the Mg-6Zn-*x*Ce (*x*=0, 0.5, 1.0, 1.5, wt.%) alloys were extruded at 300 °C and 350 °C after solution treatment. The phase constitution and microstructure evolution of Mg-Zn-*x*Ce alloys were analyzed by X-ray diffraction (XRD), scanning electron microscopy (SEM), energy dispersive spectroscopy (EDS) and electron backscattering diffraction (EBSD). Meanwhile, the mechanical properties of the alloy were tested at room temperature. For as-cast alloys, the results show that the main compound in Mg-6Zn alloy is Mg_4Zn_7 phase, and the main compound is T-$(MgZn)_{12}Ce$ phase after the addition of different amounts of Ce. The microstructure and distribution of second phases are greatly improved after extrusion at 300 °C and 350 °C. Compared with initial mechanical properties, the strength and elongation increase obviously by means of extrusion at different temperatures. In addition, the microstructure after extrusion at 350 °C is further analyzed according to EBSD data. The results show that rare earth element Ce probably promotes the activation of non-basal slip during the deformation process with the increase of Ce, which reduces the strength of basal texture and thus improves the plasticity of the alloy. Meanwhile, the increase of grain boundary migration ability leads to the gradual increase of recrystallization grain size and decreases the strength.

Keywords: Mg-Zn-Ce; extrusion; microstructure; mechanical properties; magnesium alloys

CLC numbers: TG146.22 **Document code:** A **Article ID:** 1672-6421(2023)04-271-09

1 Introduction

Magnesium and its alloys are the lightest metal structural materials, with low density, high specific strength and stiffness, favorable damping, good thermal conductivity, good electromagnetic shielding effect, excellent machining performance, stable parts size, easy recovery and other advantages, have been widely used in automotive, aviation, and aerospace fields [1, 2]. Mg-Zn magnesium alloys have been one of the research hotspots due to their high strength and good plasticity [3, 4]. However, Mg-Zn binary alloy is prone to form micropores and coarse grains, so it is not conducive to commercial casting and deformation, which greatly limits its industrial application. Alloying elements added to Mg-Zn binary alloy is an attractive method to improve the comprehensive mechanical properties of Mg-Zn alloys in industrial applications. Meanwhile, the low eutectic point temperature of Mg-Zn alloy (about 340 °C [5]) limits its high temperature application range. High melting point compounds can be formed by adding rare earth elements, which can improve the high temperature strength and creep resistance of the alloy. As an important rare earth element, Ce has a very low solid solubility in Mg [5]. When the amount of Ce is small, a large number of non-base slip systems are promoted by Ce during the deformation process, which can improve the texture distribution of the deformed magnesium alloy and significantly improve the ductility of the alloy [6-8]. When the Ce content is greater than 1%, high-temperature stable $Mg_{12}Ce$ phase is formed [9, 10]. Compared with Mg matrix, $Mg_{12}Ce$ phase has higher hardness, which can improve the strength of the alloy at room temperature and high temperature [9, 10]. Therefore, Mg-Zn-Ce alloy has the potential for further development.

The alloy prepared by gravity casting method has a series of defects such as porosity, bubble and shrinkage. At the same time, the matrix grains are coarse, and

***Wen-xin Hu**

Male, born in 1984, Ph. D. His research interests mainly focus on the microstructures and mechanical properties of magnesium alloys and aluminum alloys.

E-mail: brirehuwenxin@126.com

Received: 2022-12-26; Accepted: 2023-06-09

the coarse second phase tends to be distributed along the grain boundary. These characteristics lead to the decrease of mechanical properties of the alloy [11, 12]. The mechanical properties of magnesium alloy can be greatly improved by the plastic deformation process. Magnesium alloys with high strength, good toughness and excellent comprehensive properties can be prepared by hot extrusion. Previous studies on Mg-Zn-Ce alloy mainly focused on the improvement of the ductibility by optimizing the texture of the alloy with trace amount of Ce [13, 14]. However, there is still a lack of systematic studies on the effect of Ce content on the microstructure and properties of the deformed alloy when the Ce content is greater than 0.5%. In this study, different amounts of Ce were added on the basis of Mg-6Zn alloy, and the alloy was prepared by hot extrusion process. The effects of Ce on the microstructure and properties of Mg-Zn-Ce alloys were studied systematically at cast state, solid solution state and extrusion state. The results can provide theoretical basis and experimental support for further development of Mg-Zn-Ce alloys.

2 Experimental materials and methods

In this study, Mg-Zn alloys were prepared under the condition of a certain content of Zn (6wt.%) and different contents of rare earth element Ce (0wt.%, 0.5wt.%, 1.0wt.%, 1.5wt.%) and therefore named Mg-6Zn-*x*Ce. Firstly, the ratio of raw material required by each component was calculated according to the weight of the required magnesium alloy. Then, the pure magnesium was firstly added into the melting furnace and heated to 680 °C. After stirring, the temperature of the melting furnace was set at 720 °C. After reaching the set temperature, the pure Ce was added, and then the ingredients were fully and evenly mixed. The whole melting process was carried out under the protection of SF_6 and nitrogen. Finally, the alloy melt was poured into a mould at 680 °C and cooled in air after standing for 1 h. The composition of each alloy sample was measured by ICP and the results are listed in Table 1.

Combined with the phase diagram of Mg-Zn and Mg-Ce binary alloys [15, 16], the heat treatment system of Mg-6Zn-*x*Ce was determined. The solid solution treatment process was held at 450 °C for 10 h, followed by water cooling. In order to further improve the microstructure and mechanical properties of the cast alloys, the four alloys in this experiment were subjected to hot extrusion deformation. First, the ingot after heat treatment was processed into samples with a diameter of 40 mm and a height of 20 mm. Then, the extrusion process was proceeded at the temperature of 300 °C and 350 °C, the extrusion ratio of 16, and the extrusion rate of 0.1 mm·s^{-1}. Finally, the extruded round rods samples with diameter of 10 mm were obtained. In this study, the as-cast, solid-solution, and extruded microstructures of the alloys were observed by scanning electron microscopy, the composition of the alloy was analyzed by EDS, and the phase constitution of different alloys was analyzed by XRD. The grain orientation, texture and dislocation density of the extruded alloys were measured by electron backscattering diffraction (EBSD). Tensile tests were carried out at room temperature using the Instron universal electronic testing machine with a tensile rate of 0.5 mm·min^{-1}.

Table 1: Chemical composition of Mg-Zn-Ce magnesium alloys (wt.%)

Alloy	Composition		
	Zn	Ce	Mg
Mg-6Zn-0Ce	6.59	<0.0005	Balance
Mg-6Zn-0.5Ce	6.27	0.52	Balance
Mg-6Zn-1.0Ce	6.34	1.10	Balance
Mg-6Zn-1.5Ce	6.50	1.72	Balance

3 Results and discussion

Figure 1 shows the scanning microstructure morphology of as-cast Mg-6Zn-*x*Ce (*x*=0, 0.5, 1.0, 1.5) alloys with different Ce contents. It can be seen that when rare earth element Ce is not added to the alloy, the as-cast microstructure is composed of Mg matrix and discontinuous primary phase distributed in grain boundaries and within grains. Combined with literature [17] and XRD analysis results in Fig. 4, it can be determined that the second phase discontinuously distributed in grain boundaries is Mg_4Zn_7 phase. After adding 0.5%Ce, the microstructure of as-cast Mg-Zn-Ce alloy consists of α-Mg dendrite and network intermetallic compounds. With the Ce content increasing to 1%, the volume fraction of the second phase in the alloy increases, and some compounds distributed in the grain boundary gradually transform into a continuous network structure. When the Ce content continues to increase to 1.5%, the microstructure is significantly different from the other three alloys: the second phase formed basically presents a continuous network structure with the largest volume fraction among the four alloys.

According to the Mg-Zn phase diagram, Mg-6Zn alloy forms Mg_7Zn_3 phase under the condition of equilibrium solidification [18]. However, the cooling rate in the actual casting process is faster, which will deviate from the equilibrium solidification and form Mg_4Zn_7 phase [17, 19]. The second phase transformed from Mg_4Zn_7 phase into T-$(MgZn)_{12}Ce$ phase after adding Ce [20]. The formation of T phase is related to the low electronegativity of each element. Ce and Zn have a low electronegativity of 0.53, however, the electronegativity of Mg and Zn is 0.34 [20]. Therefore, Zn is more likely to be attracted by Ce and directly form T phase in the final solidification stage. Related studies have found that T phase is a solid solution formed after Zn element dissolves in $Mg_{12}Ce$ phase, and its crystal structure is body-centered orthogonal structure [20]. T phase is a linear compound. The formation of T phase is due to the fact that Mg atoms in the lattice of $Mg_{12}Ce$ phase are gradually replaced by Zn atoms, and the change of Mg content shows a linear decrease [21]. At the same time, the content of Zn in T-phase shows a linear increasing change [21, 22].

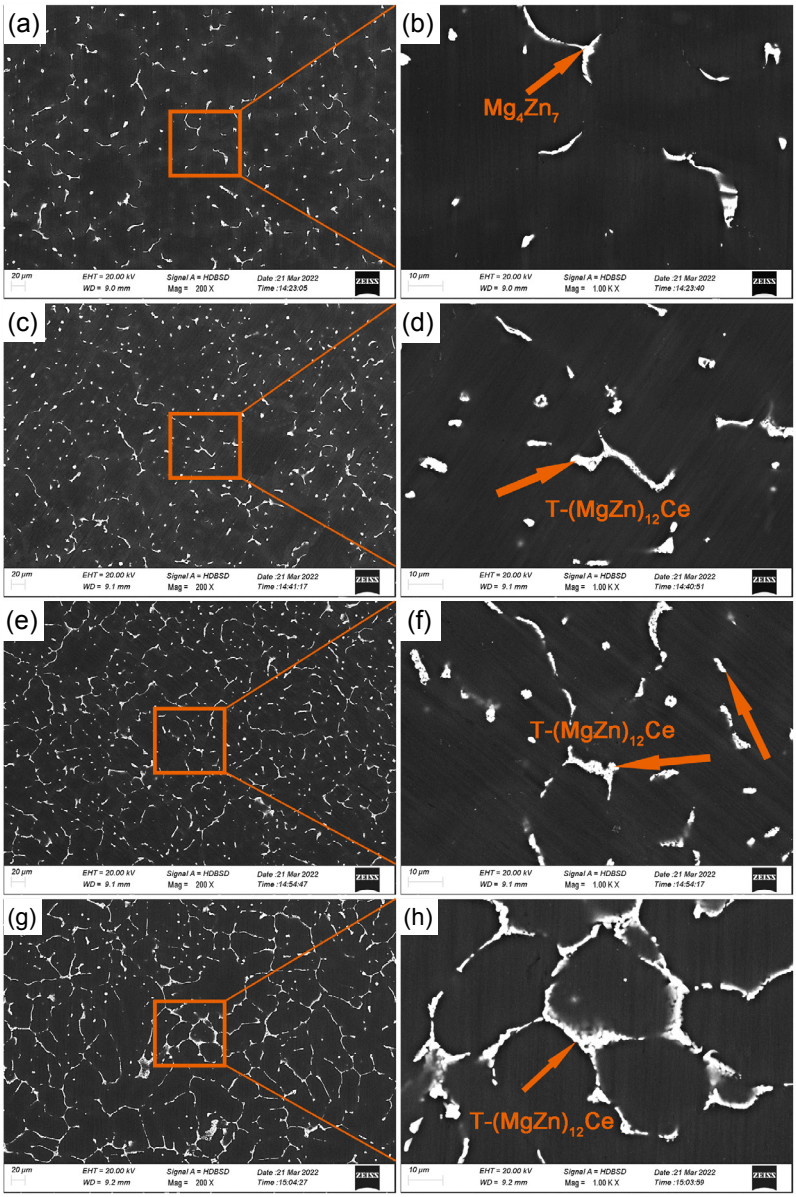

Fig. 1: SEM microstructures of as-cast Mg-6Zn-*x*Ce magnesium alloys: (a, b) *x*=0; (c, d) *x*=0.5; (e, f) *x*=1.0; (g, h) *x*=1.5

Figure 2 shows the EDS scanning analysis results of the element distribution of the as-cast Mg-6Zn-1.5Ce alloy. It can be seen that Zn and Ce elements are enriched in the grain boundary. Therefore, it can be inferred that the second phase is Mg-Zn-Ce intermetallic compound. According to relevant literature and analysis, the solid solution of Zn dissolved in the $Mg_{12}Ce$ phase will be formed in the Mg-6Zn-*x*Ce alloys, so it can be determined that the Mg-Zn-Ce intermetallic compound is T phase [9, 23].

After the solid solution treatment, it can be seen from Figs. 3(a) and (b) that the second phase Mg_4Zn_7 in the Mg-6Zn alloy is basically dissolved into the magnesium matrix, but it can be seen from Figs. 3(c) and (d) that when the Ce content is 0.5wt.%, most of the second phases will be dissolved into the matrix. The second phase changes from continuous thick strip and block to discontinuous smaller block. With the further increase of Ce content, the volume fraction and morphology change accordingly, and the continuous network T phase begins to transform into discontinuously distributed granular and massive [Figs. 3(e)(f)(g)(h)]. After the solid solution treatment, the Zn element in the T phase begins to dissolve into the magnesium matrix [Figs. 3(d)(f)(h)]. However, the solubility of Ce element in magnesium is very low, and Zn is more easily attracted by Ce, therefore, Zn element and $Mg_{12}Ce$ phase still form a linear compound T phase. As can be seen from Figs. 1(d)(f)(h) and Figs. 3(d)(f)(h), the volume fraction and morphology of T phase changes obviously compared with the as-cast state.

Figure 4 shows the XRD patterns of the as-cast and solid-solution Mg-6Zn samples after the addition of different contents of Ce element. It can be seen from Fig. 4(a) that the second phase in Mg-6Zn is Mg_4Zn_7 phase, and the second phase in the as-cast alloy is T-$(MgZn)_{12}Ce$ phase after the addition of different contents of Ce. Compared Fig. 4(b) with Fig. 1(a) and Fig. 2(a), it can be found, after the solid solution treatment, Mg_4Zn_7 phase in Mg-6Zn alloy is basically dissolved into the magnesium matrix, and the second phase in the alloy after adding rare earth is still T-$(MgZn)_{12}Ce$ phase.

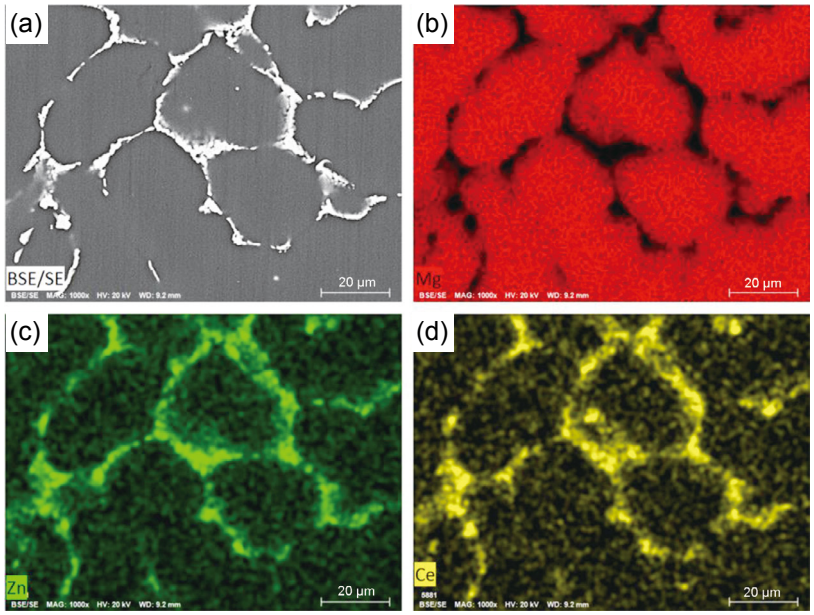

Fig. 2: EDS scanning analysis results of element distribution of as-cast Mg-6Zn-1.5Ce alloy (a–d)

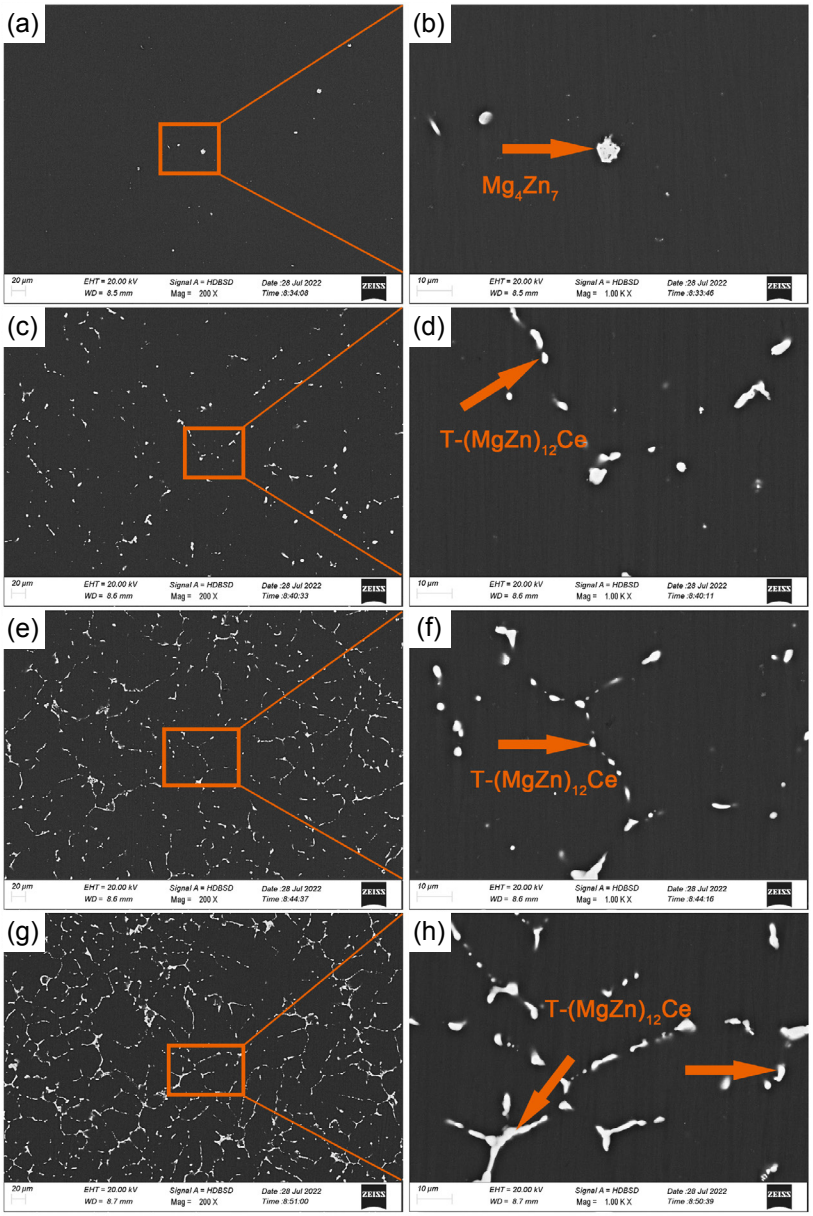

Fig. 3: SEM microstructure of Mg-6Zn-*x*Ce magnesium alloys after solid solution: (a, b) *x*=0; (c, d) *x*=0.5; (e, f) *x*=1.0; (g, h) *x*=1.5

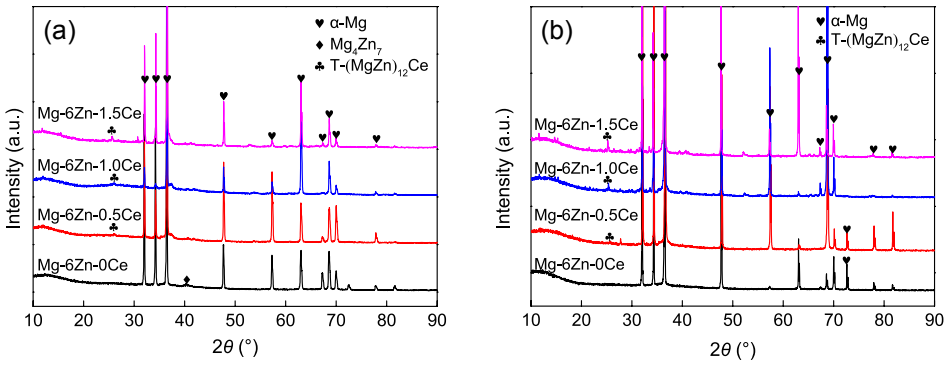

Fig. 4: XRD pattern of Mg-6Zn-*x*Ce magnesium alloys: (a) as-cast; (b) solid solution state

As can be seen from Fig. 5, after extrusion at 300 °C, the alloy without Ce has no obvious second phase precipitation. The precipitated phases of the other three alloys with different Ce contents change from irregular discontinuous block to dispersive granule, and are distributed parallel to the extrusion direction. The average size of T-$(MgZn)_{12}Ce$ precipitated phase is obviously reduced. The volume fraction of precipitated phase increases with the increase of rare earth element Ce content. When the extrusion temperature is increased to 350 °C, the evolution law of precipitated phase after extrusion is basically the same as that at 300 °C. T phase is a high melting point intermetallic compound, and it is difficult to dissolve in the alloy matrix and precipitates again during extrusion [20]. Therefore, the influence of extrusion temperature on the morphology and volume fraction of T phase does not exhibit significant changes.

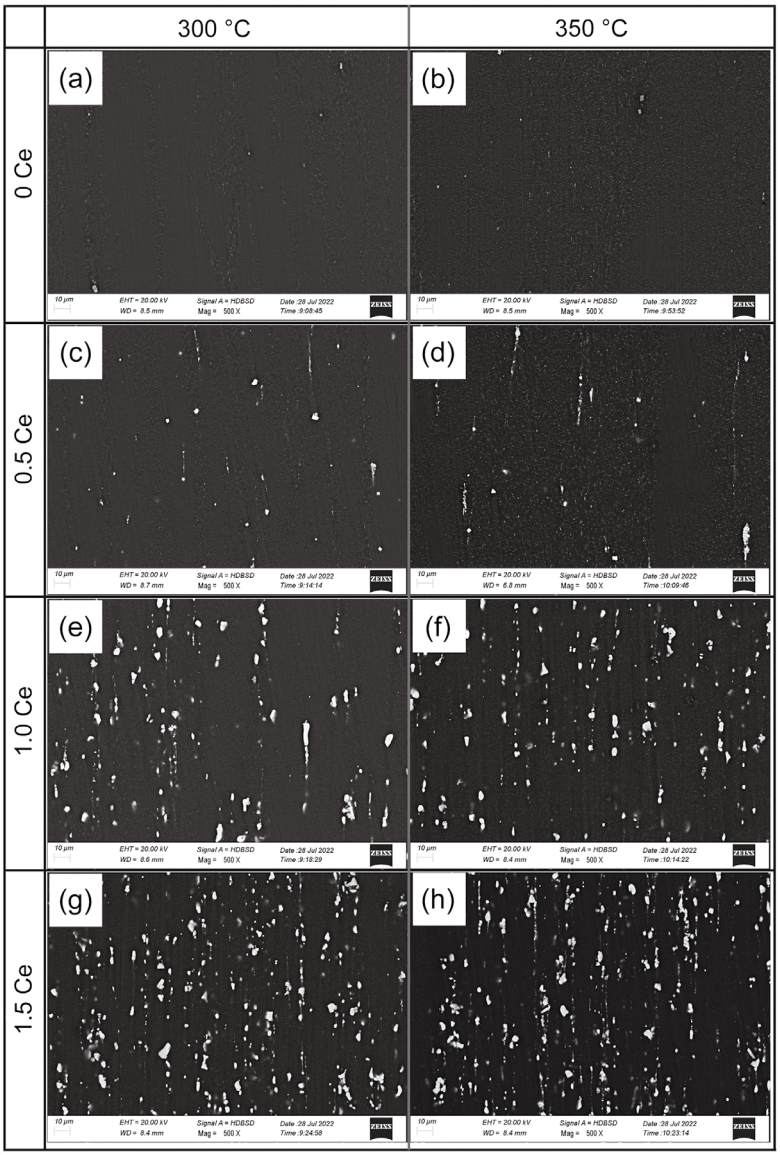

Fig. 5: SEM microstructure of Mg-6Zn-*x*Ce magnesium alloys after extrusion (a–h)

In order to explore the influence of Ce on the plastic deformation process, the EBSD tests were further conducted on the samples extruded at 350 °C. Since the strength variation of alloys after extrusion at 350 °C is more regular according to tensile test results, these samples were selected as the EBSD tests objects, and the microstructure at this temperature was further analyzed. Figure 6 shows the EBSD diagram and pole diagram of (0001), (11–20) and (10–10) of alloys with different contents of Ce after extrusion at 350 °C. EBSD diagram shows that the four magnesium alloys all undergo complete dynamic recrystallization after extrusion at 350 °C. With the change of Ce content, some grain orientations of the alloys are deflected, and the proportion of grains parallel to the extrusion direction of the base plane decreases gradually. It can also be seen from the polar diagram that the texture of the base plane is getting weaker, while the texture strength of the non-basal plane is gradually increasing. Meanwhile, it can be seen from Fig. 7 and Table 2 that with the increase of Ce content, the Schmid factor of the basal slip in Mg-6Zn-*x*Ce alloys gradually decreases. The Schmid factor of <a> prismatic slip, <a> pyramidal slip and <a+c> pyramidal slip increases gradually, which indicates that the basal slip weakens gradually and the non-basal slip increases gradually. This is due to the fact that the rare earth element Ce can reduce the critical resolved shear stress (CRSS) of the non-basal slip system, which promotes the activation of the non-basal slip system during deformation [8, 24]. Thus, the activation of a large number of non-basal slip systems during deformation promotes the homogeneous deformation of the material, which weakens the deformation texture [25].

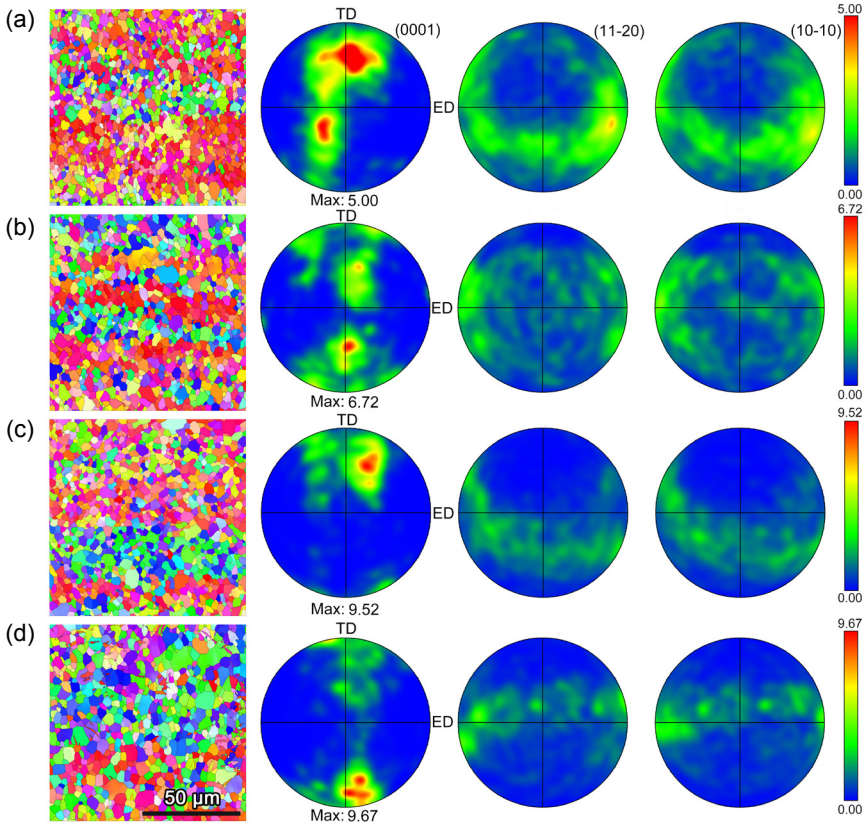

Fig. 6: IPF maps of Mg-6Zn-*x*Ce magnesium alloys after extrusion at 350 °C and polar diagrams of different crystal planes: (a) *x*=0; (b) *x*=0.5; (c) *x*=1.0; (d) *x*=1.5

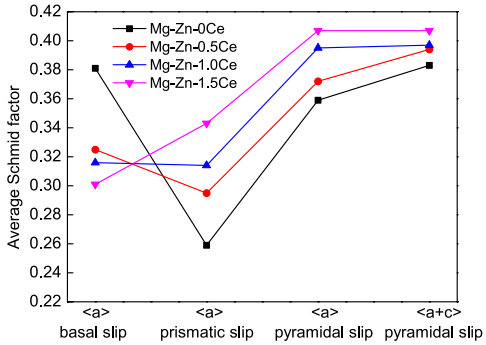

Fig. 7: Variation trend of average Schmid factors of Mg-6Zn-*x*Ce magnesium alloys in different slip systems after extrusion at 350 °C

Table 2: Average Schmid factors of Mg-6Zn-*x*Ce magnesium alloys in different slip systems after extrusion at 350 °C

Alloy	<a> basal slip	<a> prismatic slip	<a> pyramidal slip	<a+c> pyramidal slip
Mg-6Zn-0Ce	0.381	0.259	0.359	0.383
Mg-6Zn-0.5Ce	0.325	0.295	0.372	0.394
Mg-6Zn-1.0Ce	0.316	0.314	0.395	0.397
Mg-6Zn-1.5Ce	0.301	0.343	0.407	0.407

Figure 8 shows the KAM diagram and grain size distribution of Mg-6Zn-*x*Ce magnesium alloys after extrusion at 350 °C. It can be seen from Figs. 8(a), (b), (c), and (d) that the dislocation density gradually increases with the increase of Ce content, which is because Ce promotes the startup of non-basal slip system and provides more effective paths for dislocation movement, thus accumulating more dislocations. As shown in Figs. 8(e), (f), (g), and (h), with the increase of Ce content, the average size of recrystallized grains gradually increases, which is due to the increase of non-basal slip ability and grain boundary migration ability, thus promoting grain growth [26, 27]. The texture weakening effect of Ce element is mainly caused by particles which can promote nucleation. As the solid solubility of Ce in magnesium alloy is very low, it is easy to form second phase particles, and act as nucleating particles in the deformation process to promote dynamic recrystallization, thus playing a role in weakening the texture [6]. In this study, with the increase of Ce content, the volume fraction of the second phase increases, and the weakening effect on the texture of the basal plane is more obvious.

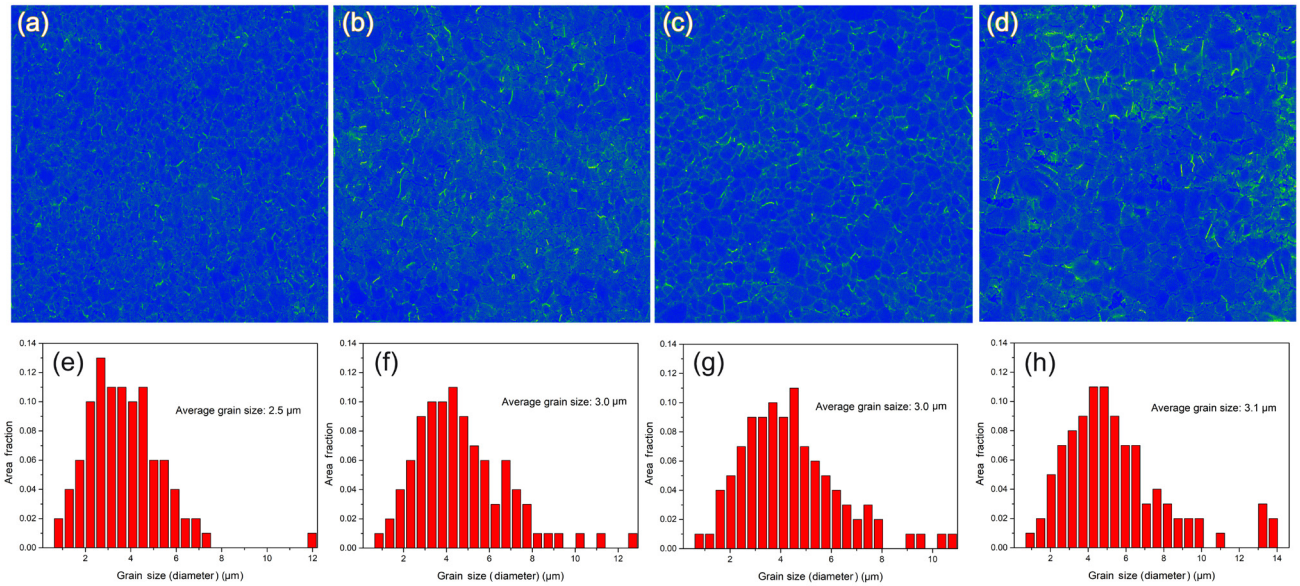

Fig. 8: KAM and grain size distribution of Mg-6Zn-*x*Ce magnesium alloys after extrusion at 350 °C: (a) and (e) *x*=0; (b) and (f) *x*=0.5; (c) and (g) *x*=1.0; (d) and (h) *x*=1.5

Figure 9 shows the room temperature tensile stress-strain curves of the Mg-6Zn-*x*Ce alloys under different states, and the values are listed in Table 3. The yield strength, tensile strength and elongation of the as-cast Mg-6Zn alloy are 90 MPa, 213 MPa, and 11.22%, respectively. After solution treatment, the strength is improved integrally, but the elongation does not change significantly.

The comprehensive mechanical properties are greatly improved after extrusion at 300 °C. For the alloy without rare earth element Ce, the yield strength, ultimate tensile strength and elongation are increased to 240 MPa, 317 MPa and 16.62%, respectively. When the Ce content is 0.5%, the elongation is as high as 22.78%, which is significantly improved compared with the as-cast state. When the extrusion temperature is increased to 350 °C, the fracture elongation is similar to 300 °C, the yield strength and ultimate tensile strength gradually decrease with the increase of Ce content. The above phenomenon is due to the fact that with the increase

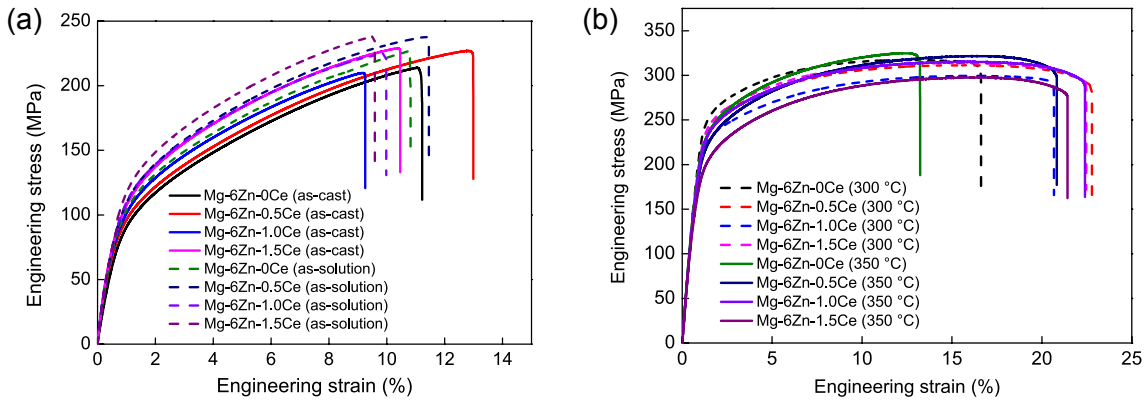

Fig. 9: Room temperature tensile stress-strain curves of Mg-6Zn-*x*Ce magnesium alloys in as-cast state, solid solution state (a) and at different extrusion temperatures (b)

Table 3: Strength and elongation of Mg-6Zn-*x*Ce under different states at room temperature

Alloy	Yield strength (MPa)	Ultimate tensile strength (MPa)	Elongation (%)
As-cast			
Mg-6Zn-0Ce	90	213	11.22
Mg-6Zn-0.5Ce	93	227	12.98
Mg-6Zn-1.0Ce	99	210	9.25
Mg-6Zn-1.5Ce	105	230	10.46
As-solution			
Mg-6Zn-0Ce	102	215	10.76
Mg-6Zn-0.5Ce	108	237	11.44
Mg-6Zn-1.0Ce	110	224	9.98
Mg-6Zn-1.5Ce	120	238	9.59
As-extruded (300 °C)			
Mg-6Zn-0Ce	240	317	16.62
Mg-6Zn-0.5Ce	220	311	22.78
Mg-6Zn-1.0Ce	215	298	20.67
Mg-6Zn-1.5Ce	229	313	22.47
As-extruded (350 °C)			
Mg-6Zn-0Ce	218	324	13.22
Mg-6Zn-0.5Ce	206	318	20.83
Mg-6Zn-1.0Ce	191	316	22.40
Mg-6Zn-1.5Ce	185	296	21.43

of Ce content, a large number of non-basal slip systems initiate, which gradually increases the recrystallization grain size and thus reduces the yield strength and ultimate tensile strength. However, the activation of non-basal slip systems weakens the texture strength of the basal plane, thus promoting the uniform plastic deformation of the material and improving the plasticity of the rare earth magnesium alloy. By analyzing the mechanical properties at room temperature, it can be seen that the influence of extrusion temperature on the strength does not have a specific rule. When the extrusion temperature is 300 °C, the strength decreases at first and then increases, while when the extrusion temperature is 350 °C, the change of strength shows a decreasing trend. For the alloy with the same composition, the yield strength decreases and the ultimate tensile strength increases firstly and then decreases with the increase of temperature. Therefore, the yield ratio decreases with the increase of temperature, and the work hardening ability increases. According to the Hall-Patch relationship, it can be inferred that grain coarsening is the main reason for the decrease of yield strength, meanwhile, grain coarsening weakens the grain boundary strengthening effect, and the yield ratio may be reduced [28].

4 Conclusions

Mg-Zn-*x*Ce alloys were prepared by adding 0.5wt.%, 1wt.% and 1.5wt.% Ce to Mg-6Zn alloy. According to analysis of the evolution rules of microstructure and mechanical properties of as-cast, as-solution and as-extruded in different alloys, the following results are obtained:

(1) In the as-cast microstructure of Mg-6Zn alloy, the main compound is Mg_4Zn_7 phase, with the addition of rare earth element Ce, the T-$(MgZn)_{12}Ce$ phase with network structure distributes continuously along the grain boundary. After solution treatment, there are still some remaining T-$(MgZn)_{12}Ce$ phases, but their volume fraction decreases and their morphology changes from thick strips and blocks to discontinuous smaller blocks. After extrusion at different temperatures, T-$(MgZn)_{12}Ce$ phase changes from irregular discontinuous massive to dispersed granular, and parallel to the extrusion direction.

(2) The strength and elongation of the four kinds of alloys after extrusion deformation increase significantly. When extrusion at 300 °C, the mechanical properties of Mg-6Zn-1.5Ce alloy are the optimal. Its yield strength, ultimate tensile strength,

and elongation are 229 MPa, 313 MPa, 22.47%, respectively. Mg-6Zn-0.5Ce exhibits excellent comprehensive mechanical properties after extrusion at 350 °C. Its yield strength, ultimate tensile strength and elongation are 206 MPa, 318 MPa, and 20.83%, respectively.

(3) For as-extruded microstructure at 350 °C, with the enhancement of Ce content, the average Schmid factor of basal slip decreases gradually. In contrast, the average Schmid factor of non-basal slip increases accordingly. The rare earth element Ce probably promotes the activation of non-basal slip during the deformation process, which reduces the texture strength of the basal plane, and increases the grain boundary migration ability. The growth of recrystallized grains leads to the decrease of strength, and the weakening of basal texture improves the plasticity of alloys.

Acknowledgements

This work was supported by the National Key Research and Development Program of China (2021YFB3501001), and the Inner Mongolia Autonomous Region Science and Technology Program (2020GG0318).

Conflict of interest

The authors declare that they have no conflict of interest.

References

[1] Yang Z, Li J, Zhang J X. Review on research and development of magnesium alloys. Acta Metallurgica Sinica (English Letters), 2008, 21(5): 313–328.
[2] Friedrich H, Schumann S. Research for a "new age of magnesium" in the automotive industry. Journal of Materials Processing Technology, 2002, 117(3): 276–281.
[3] Zhang Z Y, Huang X F, Yang F, et al. Effect of La addition on semi-solid microstructure evolution of Mg-7Zn magnesium alloy. China Foundry, 2022, 19(5): 403–410.
[4] Buha J. The effect of Ba on the microstructure and age hardening of an Mg-Zn alloy. Materials Science and Engineering: A, 2008, 491(1/2): 70–79.
[5] Kevorkov D, Pekguleryuz M. Experimental study of the Ce-Mg-Zn phase diagram at 350 °C via diffusion couple techniques. Journal of Alloys and Compounds, 2009, 478(1/2): 427–436.
[6] Chino Y, Kado M, Mabuchi M. Compressive deformation behavior at room temperature – 773 K in Mg-0.2mass% (0.035at.%)Ce alloy. Acta Materialia, 2008, 56(3): 387–394.
[7] Gao L, Yan H, Luo J, et al. Microstructure and mechanical properties of a high ductility Mg-Zn-Mn-Ce magnesium alloy. Journal of Magnesium and Alloys, 2013, 1(4): 283–291.
[8] Liu P, Jiang H, Cai Z, et al. The effect of Y, Ce and Gd on texture, recrystallization and mechanical property of Mg-Zn alloys. Journal of Magnesium and Alloys, 2016, 4(3): 188–196.
[9] Luo A A, Mishra R K, Sachdev A K. High-ductility magnesium-zinc-cerium extrusion alloys. Scripta Materialia, 2011, 64(5): 410–413.
[10] Cai J, Ma G, Liu Z, et al. Influence of rapid solidification on the mechanical properties of Mg-Zn-Ce-Ag magnesium alloy. Materials Science and Engineering: A, 2007, 456(1/2): 364–367.
[11] Chino Y, Sassa K, Mabuchi M. Texture and stretch formability of Mg-1.5mass% Zn-0.2mass% Ce alloy rolled at different rolling temperatures. Materials Transactions, 2008, 49(12): 2916–2918.
[12] Zhou T, Xia H, Chen Z H. Effect of Ce on microstructures and mechanical properties of rapidly solidified Mg-Zn alloy. Materials Science and Technology, 2011, 27(7): 1198–1205.
[13] Yi D, Wang B, Fang X, et al. Effect of rare-earth elements Y and Ce on the microstructure and mechanical properties of ZK60 alloy. Materials Science Forum, 2005, 488/489: 103–106.
[14] Mishra R K, Gupta A K, Rao P R, et al. Influence of cerium on the texture and ductility of magnesium extrusions. Scripta Materialia, 2008, 59(5): 562–565.
[15] Clark J B, Zabdyr L, Moser Z. Phase diagrams of binary magnesium alloys. ASM International, Metals Park, OH, 1988: 353–364.
[16] Nayeb-Hashemi A A, Clark J B. The Ce-Mg (cerium magnesium) system. Bulletin of Alloy Phase Diagrams, 1988, 9(2): 162–172.
[17] Gao X, Nie J. Structure and thermal stability of primary intermetallic particles in an Mg-Zn casting alloy. Scripta Materialia, 2007, 57(7): 655–658.
[18] Okamoto H. Comment on Mg-Zn (magnesium-zinc). Journal of Phase Equilibria, 1994, 15(1): 129–130.
[19] Shao G, Varsani V, Wang Y, et al. On the solidification microstructure of Mg-30Zn-2.5Y metal intermetallic alloy. Intermetallics, 2006, 14(6): 596–602.
[20] Yang W, Guo X, Lu Z. Crystal structure of the ternary Mg-Zn-Ce phase in rapidly solidified Mg-6Zn-1Y-1Ce alloy. Journal of Alloys and Compounds, 2012, 521: 1–3.
[21] Huang M, Li H, Ding H, et al. Partial phase relationships of Mg-Zn-Ce system at 350 °C. Transactions of Nonferrous Metals Society of China, 2009, 19: 681–685.
[22] Huang M, Li H, Ding H, et al. Intermetallics and phase relations of Mg-Zn-Ce alloys at 400 °C. Transactions of Nonferrous Metals Society of China, 2012, 22: 539–545.
[23] Chino Y, Huang X, Suzuki K, et al. Microstructure, texture and mechanical properties of Mg-Zn-Ce alloy extruded at different temperatures. Materialias Transactions, 2011, 52(6): 1104–1107.
[24] Mackenziea L W F, Pekguleryuzb M O. The recrystallization and texture of magnesium-zinc-cerium alloys. Scripta Materialia, 2008, 59(6): 665–668.
[25] Mishra R K, Gupta A K, Rao P R, et al. Influence of cerium on the texture and ductility of magnesium extrusions. Scripta Materialia, 2008, 59(5): 562–565.
[26] Luo A A, Mishra A A, Sachdev A K. Development of high ductility magnesium-zinc-cerium extrusion alloys. Washington, USA: The Minerals, Metals & Materials Society, 2010: 313–318.
[27] Li D, Le Q, Zhou X, et al. Study on the low mechanical anisotropy of extruded Mg-Zn-Mn-Ce-Ca alloy tube in the compression process. Journal of Magnesium and Alloys, https://doi.org/10.1016/j.jma.2022.07.001.
[28] Yu Q, Sun Y. Effect of carbon connect and microstructure on the yield-strength ratio of steel. Journal of Plasticity Engineering, 2009, 16(6): 120–126.